

# UC San Diego

## UC San Diego Previously Published Works

### Title

Changes in macrophage function modulated by the lipid environment

### Permalink

<https://escholarship.org/uc/item/96n2x2pt>

### Journal

Innate Immunity, 22(3)

### ISSN

1753-4259

### Authors

Williams, Michael R  
Cauvi, David M  
Rivera, Isabel  
et al.

### Publication Date

2016-04-01

### DOI

10.1177/1753425916633886

Peer reviewed



# HHS Public Access

Author manuscript

*Innate Immun.* Author manuscript; available in PMC 2016 November 09.

Published in final edited form as:

*Innate Immun.* 2016 April ; 22(3): 141–151. doi:10.1177/1753425916633886.

## Changes in macrophage function modulated by the lipid environment

Michael R Williams<sup>1</sup>, David M Cauvi<sup>2</sup>, Isabel Rivera<sup>1</sup>, Dennis Hawisher<sup>2</sup>, and Antonio De Maio<sup>2,3,4</sup>

<sup>1</sup>Initiative for Maximizing Student Development, University of California, San Diego, La Jolla, CA, USA

<sup>2</sup>Department of Surgery, University of California San Diego, La Jolla, CA, USA

<sup>3</sup>Department of Neurosciences, University of California San Diego, La Jolla, CA, USA

<sup>4</sup>Center for Investigations of Health and Education Disparities, University of California San Diego, La Jolla, CA, USA

### Abstract

Macrophages (M $\phi$ s) play a critical role in the defense against pathogens, orchestrating the inflammatory response during injury and maintaining tissue homeostasis. During these processes, macrophages encounter a variety of environmental conditions that are likely to change their gene expression pattern, which modulates their function. In this study, we found that murine M $\phi$ s displayed two different subpopulations characterized by differences in morphologies, expression of surface markers and phagocytic capacity under non-stimulated conditions. These two subpopulations could be recapitulated by changes in the culture conditions. Thus, M $\phi$ s grown in suspension in the presence of serum were highly phagocytic, whereas subtraction of serum resulted in rapid attachment and reduced phagocytic activity. The difference in phagocytosis between these subpopulations was correlated with the expression levels of Fc $\gamma$ R. These two cell subpopulations also differed in their responses to LPS and the expression of surface markers, including CD14, CD86, scavenger receptor A1, TLR4 and low-density lipoprotein receptor. Moreover, we found that the lipid/cholesterol content in the culture medium mediated the differences between these two cell subpopulations. Thus, we described a mechanism that modulates M $\phi$  function depending on the exposure to lipids within their surrounding microenvironment.

### Keywords

Macrophages; lipids; cholesterol; inflammation; HDL; LDL; receptors

---

Reprints and permissions: [sagepub.co.uk/journalsPermissions.nav](http://sagepub.co.uk/journalsPermissions.nav)

**Corresponding author:** Antonio De Maio, University of California San Diego, School of Medicine, 9500 Gilman Dr., #0739, La Jolla, CA 92093-073, USA. [ademaio@ucsd.edu](mailto:ademaio@ucsd.edu).

### Declaration of Conflicting Interests

The author(s) declared no potential conflicts of interest with respect to the research, authorship, and/or publication of this article.

## Introduction

Macrophages (M $\phi$ s) play a key role in immunity as APCs, modulating the inflammatory response after injury and infection, eliminating pathogens, clearing cellular debris after necrosis and up-taking apoptotic cells. Moreover, M $\phi$ s also participate in tissue remodeling during wound healing.<sup>1</sup> All of these functions are critical to maintain tissue and systemic homeostasis. M $\phi$  surface receptors are critical for their function. Thus, M $\phi$ s recognize and clear foreign particles via specific surface molecules, such as Fc receptors,<sup>2-4</sup> and pathogen components by pattern recognition receptors (PRR), such as the Toll-like receptors (TLR).<sup>5</sup> M $\phi$ s populate various organs displaying specific characteristics, such as Kupffer cells in the liver and alveolar M $\phi$ s in the lung. These tissue-resident M $\phi$ s act as sentinels of the immune system and strive to maintain homeostasis in their respective organs. For example, Kupffer cells in the liver uptake toxins and pathogens; alveolar M $\phi$ s in the lung clear dust, allergens and various microorganisms; and osteoclasts in the bone participate in bone resorption.<sup>6</sup> Even within a specific tissue population, M $\phi$ s display a large range of plasticity displayed as their ability to functionally change during various pathogenic conditions, which is often referred to as polarization.<sup>7</sup> Two initial polarization stages have been described, including classically activated (M1) and alternatively activated (M2) M $\phi$ s. These two M $\phi$  stages have been defined based on their response to specific exogenous ligands. Thus, M1 M $\phi$ s are developed in response to LPS and IFN- $\gamma$ , while M2 M $\phi$ s are established in the presence of IL-4 and IL-13.<sup>8</sup> M1 and M2 M $\phi$ s have been found to elicit pro- or anti-inflammatory phenotypes, respectively. M1 M $\phi$ s act more as scavenging cells while M2 M $\phi$ s take part in injury resolution and tissue repair,<sup>9,10</sup> displaying a higher rate of cell debris clearance.<sup>11,12</sup> Recently, it has been shown that M2 and M1M $\phi$ s represent only extreme conditions of polarization, with many more states residing within a large spectrum of plasticity. For instance, tumor-associated M $\phi$ s are now thought to be a unique polarization stage aside from M1 and M2 classification.<sup>13</sup> M $\phi$  plasticity is likely due to the exposure to various microenvironments, which has been found to be reversible.<sup>14</sup> Moreover, the tissue environment plays a role in defining functionally different subpopulations of M $\phi$ s within the same organ. For example, the release of retinoic acid from the tissue environment resulted in the establishment of functionally different subpopulations of M $\phi$ s from an apparently homogeneous initial population.<sup>15</sup> These changes in M $\phi$  subpopulations occurred at the transcriptome level, which is modulated by enhancers and secondary transcription factors.<sup>16</sup>

M $\phi$  plasticity is particularly important in the defense against invading pathogens.<sup>17,18</sup> Thus, bacterial infections such as those seen in sepsis resulted in the polarization of M $\phi$ s towards a pro-inflammatory state, which can eventually lead to tissue damage and organ failure if M $\phi$ s do not revert to a non-inflammatory condition.<sup>19,20</sup> The understanding of the mechanism that modulates the changes in M $\phi$  function during pathological conditions may lead to crucial strategies for the prevention of sepsis, injury, and other inflammatory diseases. In the present study, we showed that murine M $\phi$ s present two functionally different subpopulations during growth in culture conditions in the presence of FBS. These two subpopulations could be experimentally recapitulated by changes in the lipid/cholesterol content of the environment.

## Materials and methods

### Cell culture

J774A.1 cells (J774) from reticulum sarcoma of BALB/cN mice (ATCC, Manassas, VA, USA) were cultured in RPMI 1640 medium with L-glutamine supplemented with 10% FBS and penicillin/streptomycin, also referred to as complete medium (CM). J774 cells were grown on tissue culture (TC)-treated plastic dishes and cultured for no more than 20 passages.

### Bone marrow-derived M $\phi$ s

Bone marrow (BM) cells were isolated from femur and tibia of male CD-1 mice (6–8 wk old). After removing tissue/muscle, BM was flushed out with cold PBS supplemented with 2% heat-inactivated FBS using a 22-gauge needle. Single-cell suspensions were obtained after passing through a 22-gauge needle 4–6 times to dissociate cell clumps. Cells were then passed through a 70-mm cell strainer to remove residual clumps and centrifuged at 500 *g* for 5 min at 4°C. Cells were treated with red blood cell lysis buffer (eBioscience, San Diego, CA, USA), washed and centrifuged as described above. Isolated BM cells were re-suspended ( $2 \times 10^6$  cells/ml) in RPMI 1640 with L-glutamine and penicillin/streptomycin and supplemented with 10% FBS and 10 ng/ml recombinant M-CSF (R&D Systems, Minneapolis, MN, USA). Culture medium was changed after 3 d and non-adherent cells were discarded. On d 5, the presence of mature BM-derived M $\phi$ s was evaluated by expression of CD11b and F4/80 using fluorophore-conjugated Abs and flow cytometry. On average, >98% of the cells were CD11b<sup>+</sup> and F4/80<sup>+</sup>, corresponding to M $\phi$ s.

### Immunostaining

M $\phi$ s were seeded at  $1 \times 10^5$  cells/well on eight-chamber Lab-Tek II slides (Nunc, Roskilde, Denmark) for 2 h at 37°C, 5% CO<sub>2</sub> in either CM or serum-free (SF) RPMI 1640 medium. Cells were washed with FACS staining buffer (FSB, 0.5% BSA in DPBS without Ca<sup>2+</sup> and Mg<sup>2+</sup>) and stained with 2 mg FITC-conjugated anti-Fc $\gamma$ R (CD16/CD32) Abs (eBioscience, San Diego, CA, USA) for 1 h at 4°C. Cells were then washed with FSB, fixed for 20 min with 4% paraformaldehyde followed by another wash with FSB and mounted with vectashield (Vector Laboratories, Burlingame, CA, USA) containing DAPI. Slides were analyzed using a Nikon Eclipse TE300 fluorescent microscope equipped with Axio Cam HRm (Zeiss, Jena, Germany). For phase contrast microscopy analysis, M $\phi$ s were seeded ( $5 \times 10^4$ ) on TC-treated 96-well plates for 16 h at 37°C, 5% CO<sub>2</sub> and visualized as previously described.

### Measurement of mRNA levels using quantitative RT-PCR

RNA isolation was performed with TRIzol Reagent (Life Technologies, Grand Island, NY, USA) according to manufacturer instructions, followed by DNase treatment (DNase Treatment and Removal Kit; Life Technologies) and reverse transcription to cDNA (High Capacity cDNA Reverse Transcription Kit; Life Technologies). Quantitative RT-PCR (qRT-PCR) was performed using the standard curve method and Sybr Green chemistry (Qiagen, Valencia, CA, USA), and mRNA quantification was normalized using GAPDH as a

housekeeping gene. Pre-validated primer sets were obtained from Qiagen and included TNF- $\alpha$  (QT00104006), IL-10 (QT00106169), IL-6 (QT00098875) and IFN- $\beta$  (QT00249662).

### Flow cytometry analysis

Flow cytometry was performed using a FACSCanto II flow cytometer with FACSDiva software (BD Biosciences, San Jose, CA, USA). Data were analyzed using FlowJo software v. 7.6.4 (Tree Star, Ashland, OR, USA). M $\phi$ s ( $5 \times 10^5$  cells/tube) were fixed and permeabilized with Cytoperm/Cytofix (BD Biosciences) for 20 min at 4°C. Cells were then blocked for 15 min with 20% goat serum with or without 0.5 mg Fc $\gamma$ R blocking Abs (Fc block; BD Biosciences) followed by primary Ab staining for 30 min in the dark at 4°C. Primary Abs were added at 0.5 mg/tube and included FITC-conjugated anti-CD204 (GeneTex, San Antonio, TX, USA), APC-conjugated anti-TLR4 (eBioscience), FITC-conjugated anti-CD14 (clone: Sa2-8; eBioscience), FITC-conjugated anti-Fc $\gamma$ R (CD16/CD32; eBioscience). Low-density lipoprotein receptor (LDLr) staining was performed using 0.5 mg rabbit-anti LDLr Ab (Abcam, Cambridge, UK) followed by 0.25 mg FITC-conjugated, goat-anti-rabbit Ab (Molecular Probes, Eugene, OR, USA) for 30min in the dark at 4°C. Surface protein marker expression was expressed as the geometric mean fluorescent intensity (MFI).

### Phagocytosis analysis

The phagocytosis assay was performed by incubating M $\phi$ s ( $5 \times 10^5$  cells) with opsonized *Escherichia coli* particles labeled with pHRodo (Life Technologies) at 20:1 ratio of particles to cells for 1 h at both 4°C (negative control) and 37°C. The phagocytosis levels were expressed as the geometric MFI.

### Stimulation with LPS

LPS (1 ng/ml) was pre-incubated in 50 ml RPMI 1640 medium supplemented with 10% FBS for 30 min at 37°C to allow LPS/LPS binding protein interaction, and was added to J774 cells ( $5 \times 10^5$  cells) grown in suspension or attached for 2 h at 37°C. Cells were then washed and lysed for total RNA preparation. Cytokine mRNA levels (TNF- $\alpha$ , IL-6, IL-10 and IFN $\beta$ ) were measured by qRT-PCR using GAPDH mRNA levels to normalize the samples as described above.

### Cell cycle analysis

Cell cycle analysis was performed by fixing M $\phi$ s ( $2 \times 10^6$  cells) in 70% EtOH for 2 h at 4°C followed by treatment with propidium iodide master mix [500  $\mu$ l solution consisting of propidium iodide (Life Technologies), RNaseA (Sigma, St. Louis, MO, USA) and 0.1% Triton X-100 in DPBS without Ca $^{2+}$  or Mg $^{2+}$ ] for 15 min at 37°C. Samples were read by flow cytometry as listed above, and cell cycle data were analyzed using a Watson (Pragmatic) model with Flow Jo v. 7.6.4.

### Liposome preparation

Phosphatidylserine (PS), phosphatidylcholine (PC) phospholipids and cholesterol in chloroform were all from Avanti (Alabaster, AL, USA). Liposomes were prepared by

evaporating chloroform with nitrogen gas and re-suspending the dried lipid layer in 50mM Tris pH 7.4 for 30 min by vortexing every 5 min. Liposomes were then extruded 15 times through 100-nm filters and centrifuged at 100,000 *g* for 40 min followed by re-suspension in SF RPMI before addition to M $\phi$ s.

### Cell adhesion method

Suspension J774 cells were seeded at  $5 \times 10^4$  cells per well in non-TC-treated 96-well flat bottom plates in SF RPMI 1640 medium for 2 h with and without given treatments. Treatments included LDL, high-density lipoprotein (HDL), BSA, hemoglobin (all from Sigma), PS liposomes, PC liposomes, PC/cholesterol liposomes (1:1) and water-soluble cholesterol (Sigma). After 2 h incubation at 37°C, cells were washed once in 200  $\mu$ l DPBS (without Ca<sup>2+</sup> and Mg<sup>2+</sup>), and 0.5 mg/ml MTT solution (Sigma) was added in SF medium followed by 2 h incubation at 37°C. MTT solution was aspirated, and 100  $\mu$ l DMSO was added to dissolve crystals followed by spectrophotometric analysis at 570nm and 630nm (background).

### Statistics

Statistical analysis was performed using GraphPad Prism (San Diego, CA, USA). Significance was analyzed using two-tailed *t*-tests and one-way ANOVA. A *P*-value of <0.05 was considered statistically significant. Each experiment was performed in triplicate and repeated at least three times.

## Results

### Macrophages display two distinct subpopulations under non-stimulated conditions

Two distinct morphological subpopulations were observed by phase contrast microscopy of BM-derived M $\phi$ s isolated from CD-1 mice after 5 d of culture/differentiation. One of these subpopulations appeared 'spread', while the second subpopulation was 'round' at low-density cultures (Figure 1a). Two subpopulations of different sizes were also observed on forward scattered light (FSC) analysis by flow cytometry (Figure 1b). These two subpopulations correspond to 'smaller' and 'larger' cells, which resembled the populations observed by phase contrast microscopy. These observations led us to investigate if there were phenotypic differences between these two subpopulations. The expression levels of several surface markers, including Fc $\gamma$ R (CD16/CD32), CD14 and CD86, were elevated in the larger population of BM-derived M $\phi$ s in comparison with the smaller population (Figure 1c).

In contrast, TLR4, scavenger receptor A1 (Sra1 or Msr1) and LDLr surface levels were not different in larger and smaller BM-derived M $\phi$ s, as observed by flow cytometry (Figure 1c). Similar observations were made on J774 cells, which correspond to a murine M $\phi$  line by phase contrast microscopy (Figure 2a) and flow cytometry (Figure 2b), resembling the small and large subpopulations observed in BM-derived M $\phi$ s. The appearance of these two subpopulations in J774 cells was not affected by the density of cells in the culture. In addition, these two subpopulations were not due to differences in the cell cycle (Figure 2c). A comparison of surface markers within the two subpopulation of J774 cells also display

elevated levels of Fc $\gamma$ R (CD16/CD32), CD14 and CD86 in the larger cell subpopulation as opposed to the smaller cells. In contrast, TLR4 was significantly higher on the smaller cells in comparison with the larger cells, as observed by flow cytometry. Other surface proteins, including Sra1 LDLr, showed no difference between the two subpopulations (Figure 2d).

We also assessed whether these cell subpopulations displayed differences in function. As phagocytosis plays a major role in macrophage function and we have observed differences in Fc $\gamma$ R levels, we investigated whether or not Fc-mediated phagocytosis was different between these two subpopulations. Indeed, phagocytosis of opsonized particles was significantly higher in the larger cell subpopulation of BM-derived M $\phi$ s compared with the smaller cells, as detected by flow cytometry (Figure 3a). These observations regarding differences in phagocytosis were also observed in J774 cells (Figure 3b).

### **Macrophage subpopulations are recapitulated by changes in the growing environment**

We observed that J774 M $\phi$ s could be grown in suspension on non-TC-treated plastic dishes, displaying a phenotype like the round/large cells observed in regular TC dishes (Figure 4a). Analysis of these cells in suspension by flow cytometry demonstrated that they grew as a homogenous population, and their size was similar to the subpopulation of round cells observed in TC dishes (Figure 4b). When suspension cells (S) were exposed to SF conditions for a very short time, they rapidly and firmly attached and spread onto non-TC dishes (Figure 4c). The attached cells (A) in serum-free conditions also resulted in a homogenous population as observed by flow cytometry (Figure 4d), resembling the size of the small population observed in the original TC conditions. In summary, cells in suspension correspond to the round and larger population whereas attached cells are spread and smaller. These observations also suggest that changing the culture environment alters M $\phi$  phenotype.

The attachment to non-TC dishes of suspension cells in absence of serum was observed to occur rapidly within 5min after serum removal, reaching a plateau within 30 min (Figure 5a). The attachment percentage of suspension cells was inversely proportional to the concentrations of FBS added (Figure 5b). Next, we investigated the possible specific component in serum that could modulate the attachment. Addition of BSA to suspension cells in absence of FBS resulted in prevention of attachment onto non-TC plates (Figure 5c). Other proteins, such as hemoglobin (Hb), did not inhibit the attachment of S cells in serum-free conditions (Figure 5d). The addition of either LDL or HDL also significantly prevented attachment of cells to non-TC dishes (Figure 5e,f). As BSA is known to carry both fatty acids and cholesterol, and HDL and LDL contain both phospholipids and cholesterol,<sup>21</sup> we investigated the effect of specific lipids on cell attachment. Cells in suspension in FBS-free medium were incubated with either liposomes made of PS or PC phospholipids. Both PS and PC liposomes had no effect on macrophage attachment (Figure 5g). However, water-soluble cholesterol had a drastic effect on the attachment of macrophages, significantly decreasing their adherence to non-TC dishes (Figure 5h). To confirm the specific effect of cholesterol, we prepared PC liposomes with and without a physiological concentration of cholesterol and incubated with suspension cells in FBS-free conditions. We found that the attachment of suspension cells was also significantly reduced upon incubation with cholesterol PC-liposomes but not with PC-liposomes without cholesterol (Figure 5i). In



summary, our results showed that M $\phi$ s adhere very rapidly to non-TC dishes in the absence of serum, and the lack of cholesterol may be responsible for this effect, although other factors within serum may be involved.

### Suspension and attached macrophages have different phenotypes and functions

The subpopulations of M $\phi$ s with distinct sizes and morphologies were further analyzed for protein expression, phagocytic activity and response to LPS. Initially, we assessed whether S or A J774 cells showed any differences in the stages of their cell cycles as serum starvation has been shown to induce cell cycle arrest of cells into the G<sub>0</sub>/G<sub>1</sub> phase.<sup>22</sup> We did not observe any differences in the cell cycle between S or A subpopulations, most likely due to the short length of serum-free conditions (Figure 6a). Expression of CD86, CD14, Sra1 and Fc $\gamma$ R were significantly higher in suspension M $\phi$ s compared with attached cells, while TLR4 and LDLr were significantly higher in attached M $\phi$ s as opposed to suspension cells (Figure 6b). Typical markers of M1 and M2 M $\phi$ s, such as iNOS (M1) and Arg1 (M2), were also analyzed by qRT-PCR. The expression of iNOS mRNA was elevated in suspension cells as opposed to attached cells, whereas no differences were observed at the level of Arg1 mRNA levels (Figure 6c). Fc-mediated phagocytosis was also significantly higher in suspension M $\phi$ s compared with attached cells (Figure 6d). Finally, each population of M $\phi$ s reacted differently to LPS treatment. Both populations were incubated with LPS (1 ng/ml) for 2 h in the presence of serum, and the expression of several cytokines was measured by qRT-PCR. The mRNA levels of TNF- $\alpha$ , IL-6 and IFN- $\beta$  were significantly higher in A M $\phi$ s compared with S cells. On the contrary, IL-10 mRNA expression levels were significantly increased in suspension M $\phi$ s as opposed to attached cells (Figure 6e). The difference in LPS response between the two populations revealed that attached cells have a pro-inflammatory phenotype as opposed to the anti-inflammatory phenotype of suspension cells. This observation demonstrates another distinct functional difference between the two populations.

### Discussion

M $\phi$ s are key players in both innate and adaptive immune responses. These cells clear pathogens, cell debris produced after necrosis and apoptotic cells. In addition, M $\phi$ s release molecules necessary for the inflammatory response. M $\phi$ s also participate in the adaptive immune response by acting as APCs. M $\phi$ s are distributed among different organs to participate in all of these processes, and they have the ability to migrate into sites of injury, contributing to tissue recovery and remodeling. During these processes, M $\phi$ s encounter different physiological and nutritional environments, resulting in functional changes that are often referred to as polarization,<sup>7,14</sup> which is likely the product of changes in gene expression.<sup>16</sup> In the present study, we showed that murine M $\phi$ s presented two distinct subpopulations under normal conditions, each with unique morphologies and displaying differences in function. The two subpopulations of M $\phi$ s observed in this study differ in size and shape, large/round and small/spread, and the presence of specific surface markers, such as CD14 and CD86, which did not depend on the cell confluency. These observations echo prior reports describing two distinct subpopulations of peritoneal M $\phi$ s isolated from naïve BALB/c mice.<sup>23</sup> However, further studies are needed to investigate whether or not



subpopulations of M $\phi$ s observed *in vivo* displayed functional differences, such as phagocytosis.

The characteristics of these two subpopulations, large/round and small/spread, could be recapitulated by the environmental conditions, in particular by the cholesterol concentration within the medium. Indeed, specific homogenous populations that displayed different protein markers and functions could be obtained by changes in the culture conditions and cholesterol concentration within medium. Thus, M $\phi$ s grown in suspension in the presence of serum displayed a round morphology, a robust phagocytic activity and higher expression of anti-inflammatory cytokines after stimulation with LPS. When these cells in suspension were exposed to serum-free conditions, they became very adherent to non-TC dishes and presented a 'fibroblast-like' shape with reduced phagocytic capacity and an up-regulation of pro-inflammatory cytokines after incubation with LPS. Prior studies have shown that the external environment modulates M $\phi$  function. M $\phi$ s exposed to an external acidic environment, similar to that encountered during infection, resulted in an increase of the phagocytic capacity of M $\phi$ s.<sup>24</sup> The effect of an acidic microenvironment on M $\phi$  function was also described at the level of LPS-induced cytokine production in culture conditions,<sup>25</sup> as well as in *in vivo* conditions.<sup>26</sup> Retinoic acid derived from the peritoneal omentum induced changes in gene expression in specific subpopulations of M $\phi$ s.<sup>15</sup> The effect of the environment in M $\phi$  function is modulated at the level of the transcriptome, by enhancers and secondary transcription factors.<sup>16</sup> Similarly, the expression pattern of M $\phi$  populations is associated to their bioenergetics profile.<sup>27</sup> Finally, the tumor environment has been shown to modulate the plasticity of local M $\phi$ s.<sup>13</sup>

The natural subpopulations of M $\phi$ s observed in our study could be recapped by exposure to different concentrations of lipoproteins and cholesterol in the medium. Thus, cells became less adherent when exposed to BSA, which has a great capacity to bind lipids but not to other proteins such as Hb. HDL and LDL, which contained both phospholipids and cholesterol, also affected M $\phi$  attachment. Finally, cholesterol, water soluble or associated with phospholipids, appeared responsible for decreasing adherence. Therefore, we proposed that the presence of cholesterol in the environment plays a significant role in M $\phi$  plasticity. The effect of cholesterol on M $\phi$  function has been often associated with their role in the development of atherosclerosis. In this regard, M $\phi$ s become foam cells as the product of an excessive influx of cholesterol into the cell via modified LDL, such as oxidized LDL, or through the uptake of large amounts of native LDL by pinocytosis.<sup>28,29</sup> This uptake of cholesterol in excess gives M $\phi$ s a distinct phenotype related to the presence of 'lipid droplets' within the cytosol.<sup>30</sup> We found that when treating M $\phi$ s in suspension with various concentrations of LDL and water-soluble cholesterol, they did not display the presence of cytosolic 'lipid droplets'. Therefore, we do not believe that we are dealing with foam cell formation, probably because the concentration of native LDL used in our studies was much lower, less than 100 mg/ml, than the concentration used to differentiate the cells in culture, which is in the order of 2–4 mg/ml.<sup>31</sup>

We also observed an effect on the response to LPS and cytokine production after changing the cholesterol microenvironment of M $\phi$ s. Thus, cells grown in suspension in the presence of serum showed high expression levels of IL-10 and reduced levels of TNF- $\alpha$  and IL-6,



In summary, we found that a change in the external milieu of macrophages, in particular at the level of lipid content, resulted in a change of M $\phi$  function. Thus, M $\phi$ s may encounter a different environment within a tissue where the extracellular lipid content may be different than from cells in circulation, which is likely to modify their function toward clearance and resolution. Our observations might also shed light onto the mechanisms by which M $\phi$ s recruited from the blood stream become more adherent once they enter the tissue with reduced serum levels.

## Acknowledgments

### Funding

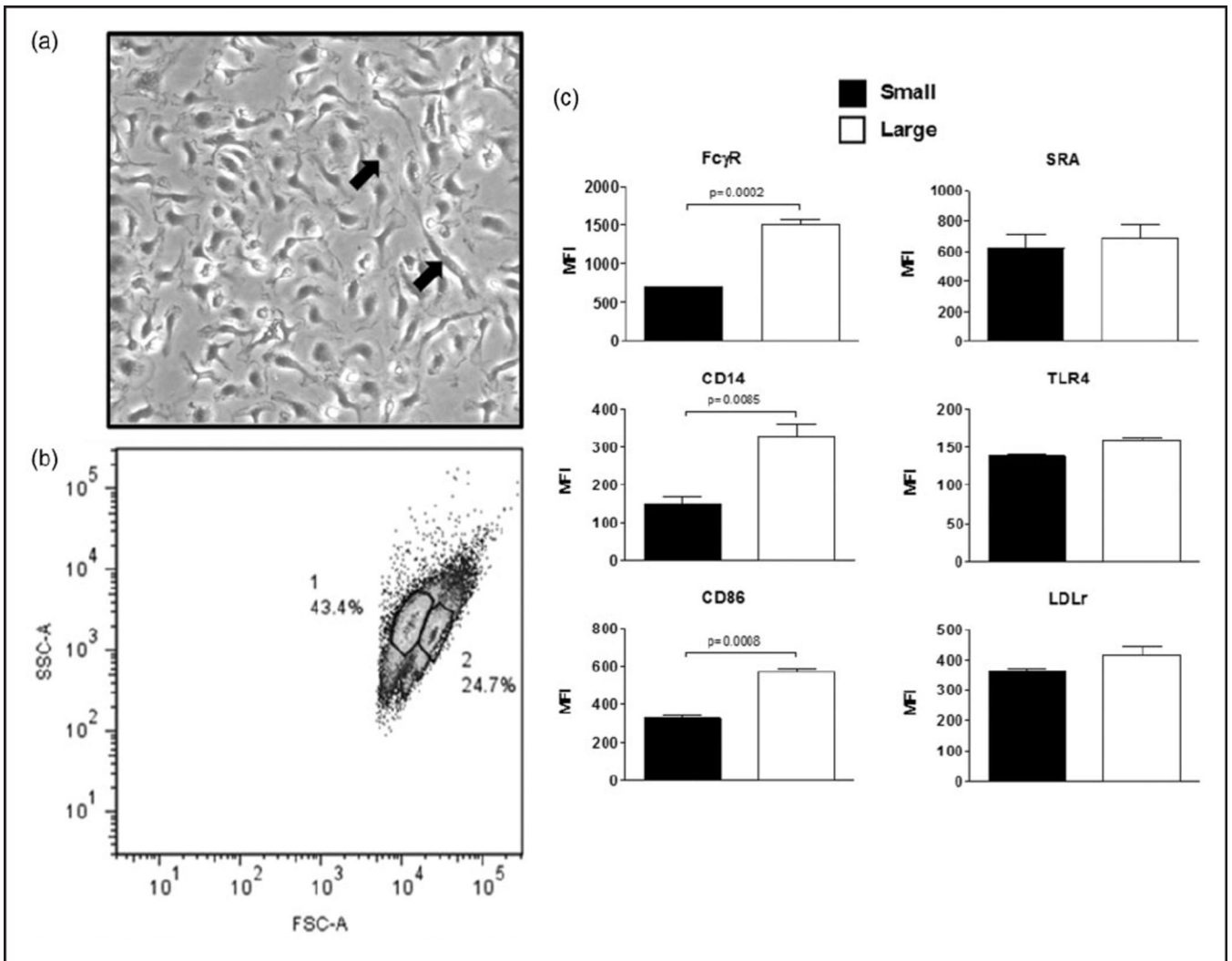
The author(s) disclosed receipt of the following financial support for the research, authorship, and/or publication of this article: This work was supported by National Institutes of Health grant numbers GM114473 and GM083275.

## References

1. Mantovani A, Biswas SK, Galdiero MR, et al. Macrophage plasticity and polarization in tissue repair and remodeling. *J Pathol.* 2013; 229:176–185. [PubMed: 23096265]
2. Flannagan RS, Jaumouille V, Grinstein S. The cell biology of phagocytosis. *Annu Rev Pathol.* 2012; 7:61–98. [PubMed: 21910624]
3. Zhang X, Mosser DM. Macrophage activation by endogenous danger signals. *J Pathol.* 2008; 214:161–168. [PubMed: 18161744]
4. Taylor PR, Martinez-Pomares L, Stacey M, et al. Macrophage receptors and immune recognition. *Ann Rev Immunol.* 2005; 23:901–944. [PubMed: 15771589]
5. Beutler B. Microbe sensing, positive feedback loops, and the pathogenesis of inflammatory disease. *Immunological Rev.* 2009; 227:248–263.
6. Murray PJ, Wynn TA. Protective and pathogenic functions of macrophage subsets. *Nat Rev Immunol.* 2011; 11:723–737. [PubMed: 21997792]
7. Mosser DM, Edward JP. Exploring the full spectrum of macrophage activation. *Nat Rev Immunol.* 2008; 8:958–969. [PubMed: 19029990]
8. Lawrence T, Natoli G. Transcriptional regulation of macrophage polarization: enabling diversity with identity. *Nat Rev Immunol.* 2011; 11:750–761. [PubMed: 22025054]
9. Rey-Giraud F, Hafner M, Ries CH. In vitro generation of monocyte-derived macrophages under serum-free conditions improves their tumor promoting function. *PLOS ONE.* 2012; 7:1–10.
10. Ho VW, Sly LM. Derivation and characterization of murine alternatively activated (M2) macrophages. *Methods Mol Biol.* 2009; 531:173–185. [PubMed: 19347318]
11. Leidi M, Gotti E, Bologna L, et al. M2 macrophages phagocytose rituximab-opsonized leukemic targets more effectively than M1 cells in vitro. *J Immunol.* 2009; 182:4415–4422. [PubMed: 19299742]
12. Vivers S, Heasman SJ, Hart SP, Dransfield I. Divalent cation-dependent and -independent augmentation of macrophage phagocytosis of apoptotic neutrophils by CD44 Ab. *Clin Exp Immunol.* 2004; 138:447–452. [PubMed: 15544621]
13. Biswas SK, Gangi L, Paul S, et al. A distinct and unique transcriptional program expressed by tumor-associated macrophages (defective NF- $\kappa$ B and enhanced IRF-3/STAT1 activation). *Blood.* 2006; 107:2112–2122. [PubMed: 16269622]
14. Stout RD, Suttles J. Functional plasticity of macrophages: reversible adaptation to changing microenvironments. *J Leukoc Biol.* 2004; 76:509–513. [PubMed: 15218057]
15. Okabe Y, Medzhitov R. Tissue-specific signals control reversible program of localization and functional polarization of macrophages. *Cell.* 2014; 157:832–844. [PubMed: 24792964]

16. Gosselin D, Link VM, Romanoski CE, et al. Environment drives selection and function of enhancers controlling tissue-specific macrophage identities. *Cell*. 2014; 159:1327–1340. [PubMed: 25480297]
17. Davis MJ, Tsang TM, Qiu Y, et al. Macrophage M1/M2 polarization dynamically adapts to changes in cytokine microenvironments in *Cryptococcus neoformans* infection. *MBio*. 2013; 4:e00264–13.
18. Hazlett LD, McClellan SA, Barrett RP, et al. IL-33 shifts macrophage polarization, promoting resistance against *Pseudomonas aeruginosa* keratitis. *Invest Ophthalmol Vis Sci*. 2010; 51:1524–1532. [PubMed: 19892870]
19. Benoit M, Desnues B, Mege JL. Macrophage polarization in bacterial infections. *J Immunol*. 2008; 181:3733–3739. [PubMed: 18768823]
20. Hotchkiss RS, Karl IE. The pathophysiology and treatment of sepsis. *N Engl J Med*. 2003; 348:138050.
21. Meierhofer T, van den Elsen JM, Cameron PJ, et al. The interaction of serum albumin with cholesterol containing lipid vesicles. *J Fluoresc*. 2010; 20:371–376. [PubMed: 19644737]
22. Chen M, Huang J, Yang X, et al. Serum starvation induced cell cycle synchronization facilitates human somatic cells reprogramming. *PLOS ONE*. 2012; 7:1–9.
23. Ghosn EEB, Cassado AA, Govoni GR, et al. Two physically, functionally, and developmentally distinct peritoneal macrophage subsets. *PNAS*. 2010; 107:2568–2573. [PubMed: 20133793]
24. Grabowski JE, Vega VL, Talamini MA, De Maio A. Acidification enhances peritoneal macrophage phagocytic activity. *J Surg Res*. 2008; 147:206–211. [PubMed: 18498871]
25. Grabowski J, Vazquez DE, Costantini T, et al. Tumor necrosis factor expression is ameliorated after exposure to an acidic environment. *J Surg Res*. 2012; 173:127–134. [PubMed: 20888586]
26. Hanly EJ, Aurora AA, Shih SP, et al. Peritoneal acidosis mediates immunoprotection in laparoscopic surgery. *Surgery*. 2007; 142:357–364. [PubMed: 17723887]
27. Izquierdo E, Delgado Cuevas V, Fernández-Arroyo S, et al. Reshaping of human macrophage polarization through modulation of glucose catabolic pathways. *J Immunol*. 2015; 195:2442–2451. [PubMed: 26209622]
28. Weber C, Neels H. Atherosclerosis: current pathogenesis and therapeutic options. *Nat Med*. 2011; 17:1410–1422. [PubMed: 22064431]
29. McLaren JE, Michael DR, Ashlin TG, Ramji DP. Cytokines, macrophage lipid metabolism and foam cells: implications for cardiovascular disease therapy. *Prog Lipid Res*. 2011; 50:331–347. [PubMed: 21601592]
30. Mori M, Itabe H, Higashi Y, et al. Foam cell formation containing lipid droplets enriched with free cholesterol by hyperlipidemic serum. *J Lipid Res*. 2001; 42:1771–1781. [PubMed: 11714846]
31. Kruth HS, Huang W, Ishil I, Zhang WY. Macrophage foam cell formation with native low density lipoprotein. *J Biol Chem*. 2002; 277:34573–34580. [PubMed: 12118008]
32. McCoy MW, Moreland SM, Detweiler CS. Hemophagocytic macrophages in murine typhoid fever have an anti-inflammatory phenotype. *Infect Immun*. 2012; 80:3642–3649. [PubMed: 22868497]
33. Frey T, De Maio A. Increased expression of CD14 in macrophages after inhibition of the cholesterol biosynthetic pathway by lovastatin. *Mol Med*. 2007; 13:592–604. [PubMed: 17932552]
34. Sandanger Ø, Ryan L, Bohnhorst J, et al. IL-10 enhances MD-2 and CD14 expression in monocytes and the proteins are increased and correlated in HIV-infected patients. *J Immunol*. 2009; 182:588–595. [PubMed: 19109192]
35. Goldstein JL, Brown MS. The LDL receptor. *Arterioscler Thromb Vasc Biol*. 2009; 29:431–438. [PubMed: 19299327]
36. Loike JD, Shabtai DY, Neuhut R, et al. Statin inhibition of Fc receptor-mediated phagocytosis by macrophages is modulated by cell activation and cholesterol. *Arterioscler Thromb Vasc Biol*. 2004; 24:2051–2056. [PubMed: 15345508]
37. Bigler RD, Khoo M, Lund-Katz S, et al. Identification of low density lipoprotein as a regulator of Fc receptor-mediated phagocytosis. *Proc Natl Acad Sci U S A*. 1990; 87:4981–4985. [PubMed: 2367519]

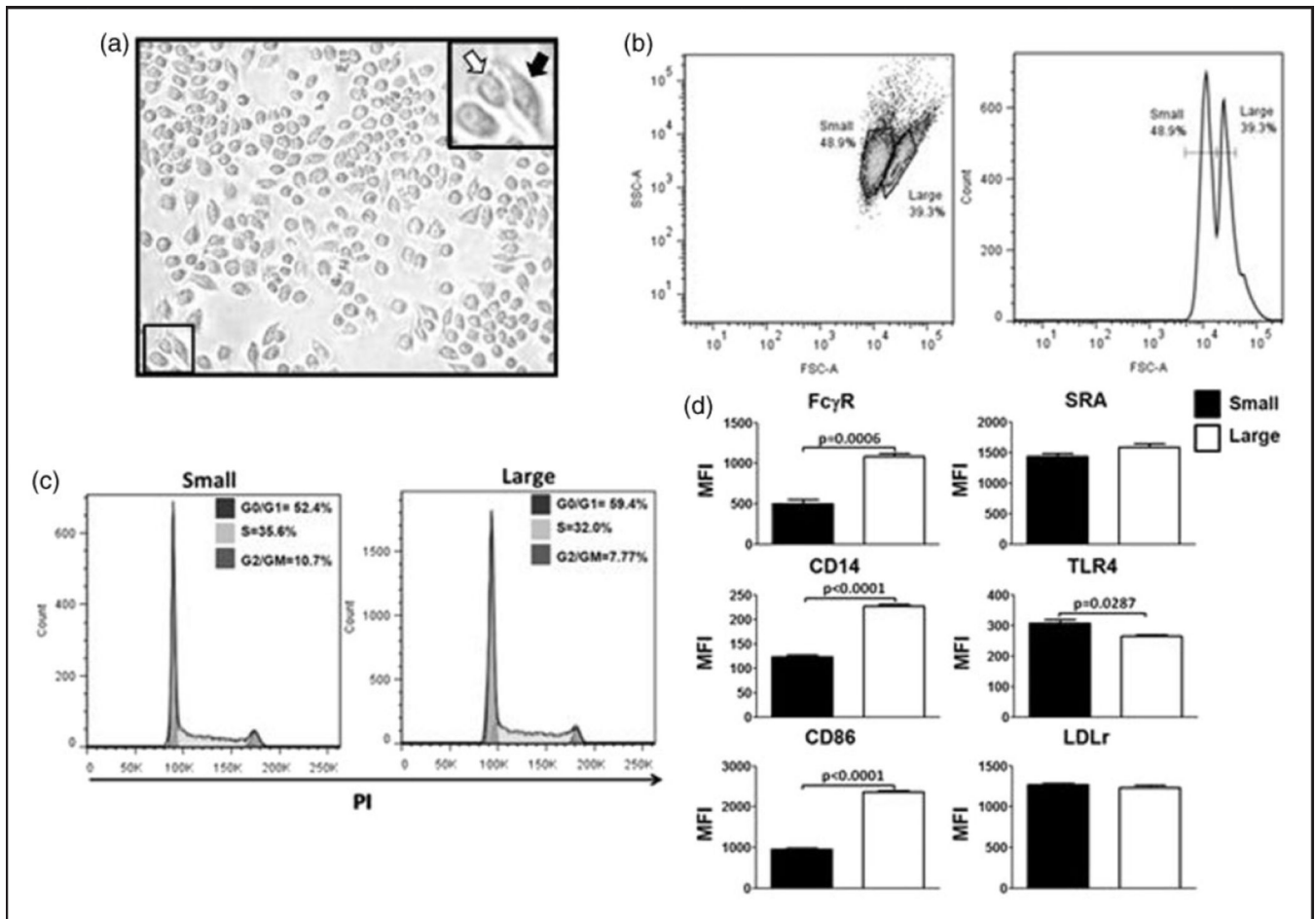
38. Nino DF, Cauvi DM, De Maio A. Itraconazole, a commonly used antifungal, inhibits Fcγ receptor-mediated phagocytosis: alteration of Fcγ receptor glycosylation and gene expression. *Shock*. 2014; 42:52–59. [PubMed: 24667630]
39. Ingber D. How cells (might) sense microgravity. *FASEB J*. 1999; 13:4–15.
40. Patel NR, Bole M, Chen C, et al. Cell elasticity determines macrophage function. *PLOS ONE*. 2012; 7:1–10.
41. Jones GE. Cellular signaling in macrophage migration and chemotaxis. *J Leukoc Biol*. 2000; 68:593–602. [PubMed: 11073096]
42. Williams LM, Ridley AJ. Lipopolysaccharide induces actin reorganization and tyrosine phosphorylation of Pyk2 and paxillin in monocytes and macrophages. *J Immunol*. 2000; 164:2028–2036. [PubMed: 10657655]
43. Swan R, Chung CS, Ayala A. Sepsis differentially affects macrophage clearance of apoptotic thymocytes. *Shock*. 2006; 25:77–78.
44. Lopez NE, Krzyzaniak M, Costantini TW, et al. Vagal nerve stimulation blocks peritoneal macrophage inflammatory responsiveness after severe burn injury. *Shock*. 2012; 38:294–300. [PubMed: 22683732]



**Figure 1.**

BM-derived macrophages present two morphologically different subpopulations. BM-derived M $\phi$ s 5 d after extraction from femur and tibia were grown on TC-treated plastic dishes in the presence of serum and recombinant M-CSF (10 ng/ml). (a) They were analyzed for morphological changes by phase contrast microscopy, presenting two subpopulations with different morphologies, round (white arrow) and spread (black arrow). (b) These two subpopulations were also observed by flow cytometry. (c) The expressions of Fc $\gamma$ R, CD14, CD86, LDLr, TLR4 and SRA were determined by flow cytometry in the sub-populations. Statistical analysis was determined by two-tailed *t*-tests from three independent experiments, and significance was accepted as  $P < 0.05$ .

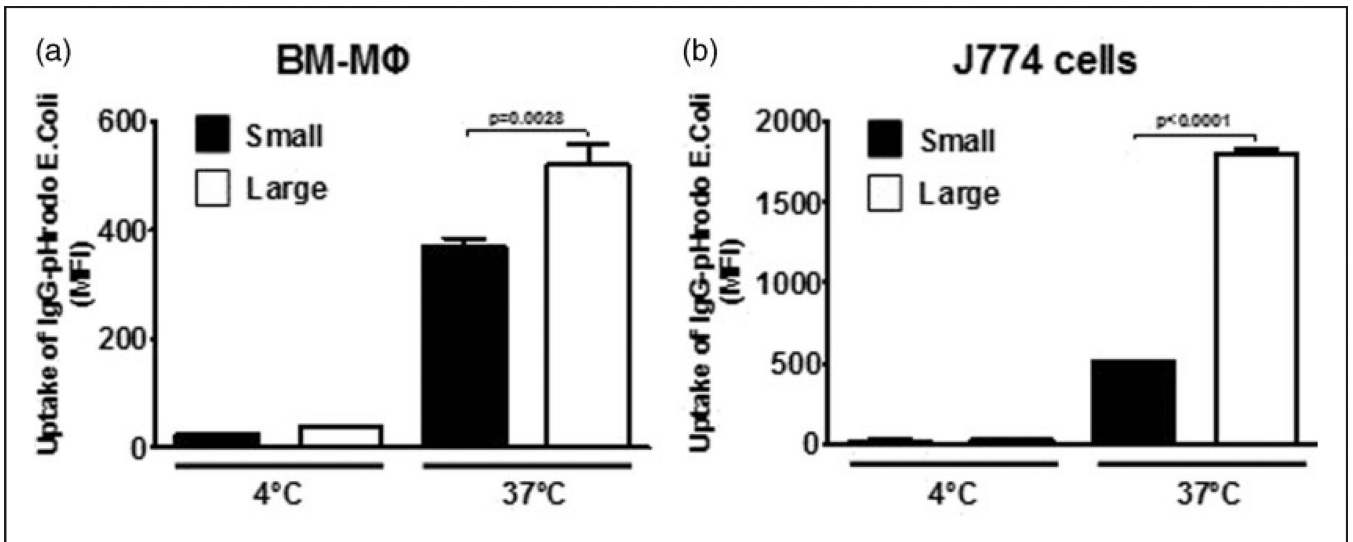




**Figure 2.**

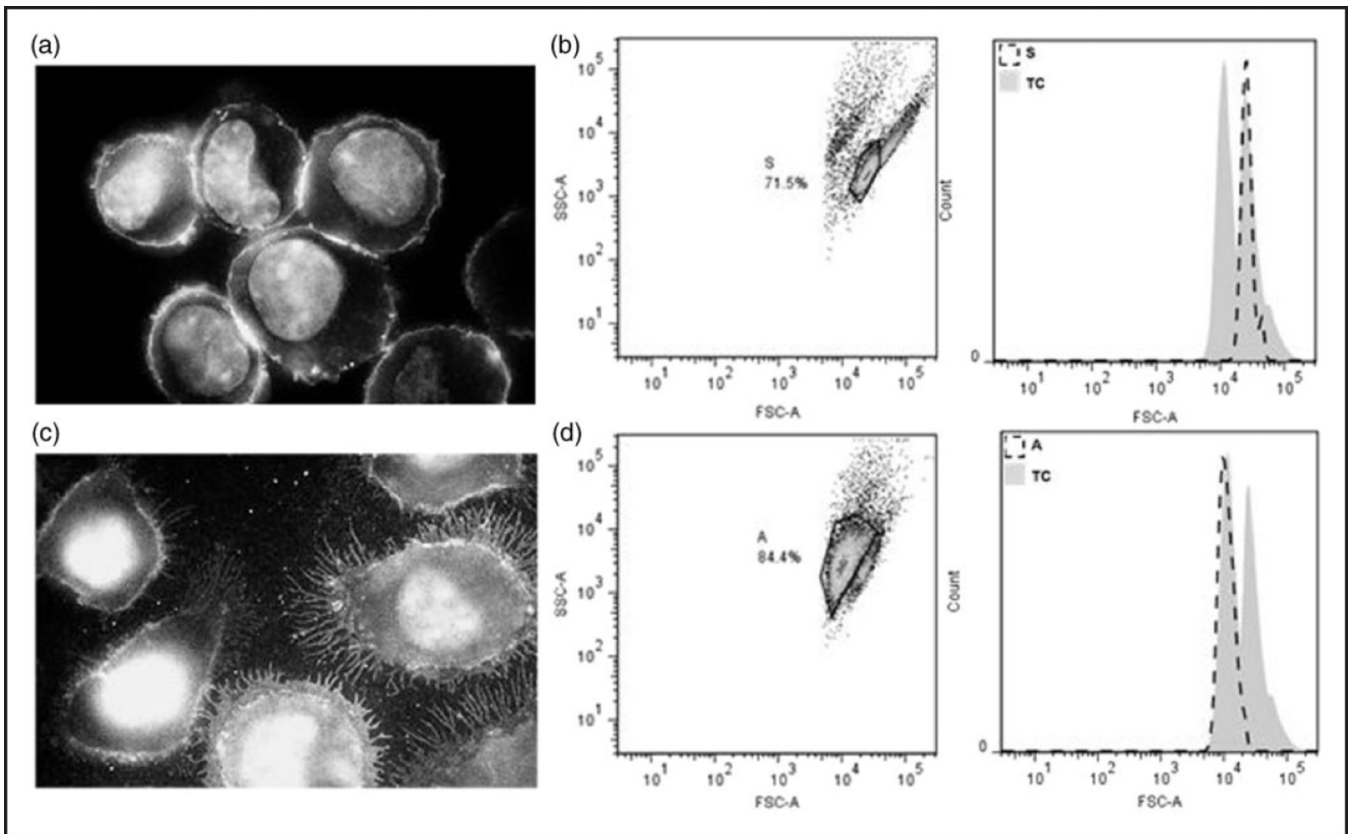
Macrophages (J774 cells) in TC conditions displayed two distinct populations. (a) Mφs (J774 cells) were grown on TC-treated plastic dishes and analyzed by phase contrast microscopy, displaying two subpopulations with different morphologies, round (white arrow) and spread (black arrow) morphology. (b) Cells were then scraped and analyzed by flow cytometry, showing two subpopulations of different size (FSC). (c) Cell cycle analysis of the two subpopulations was detected by PI staining and flow cytometry. (d) The expressions of FcγR, CD14, CD86, LDLr, TLR4 and SRA were determined by flow cytometry in the subpopulations. Statistical analysis was determined by two-tailed *t*-tests from three independent experiments, and significance was accepted as  $P < 0.05$ .





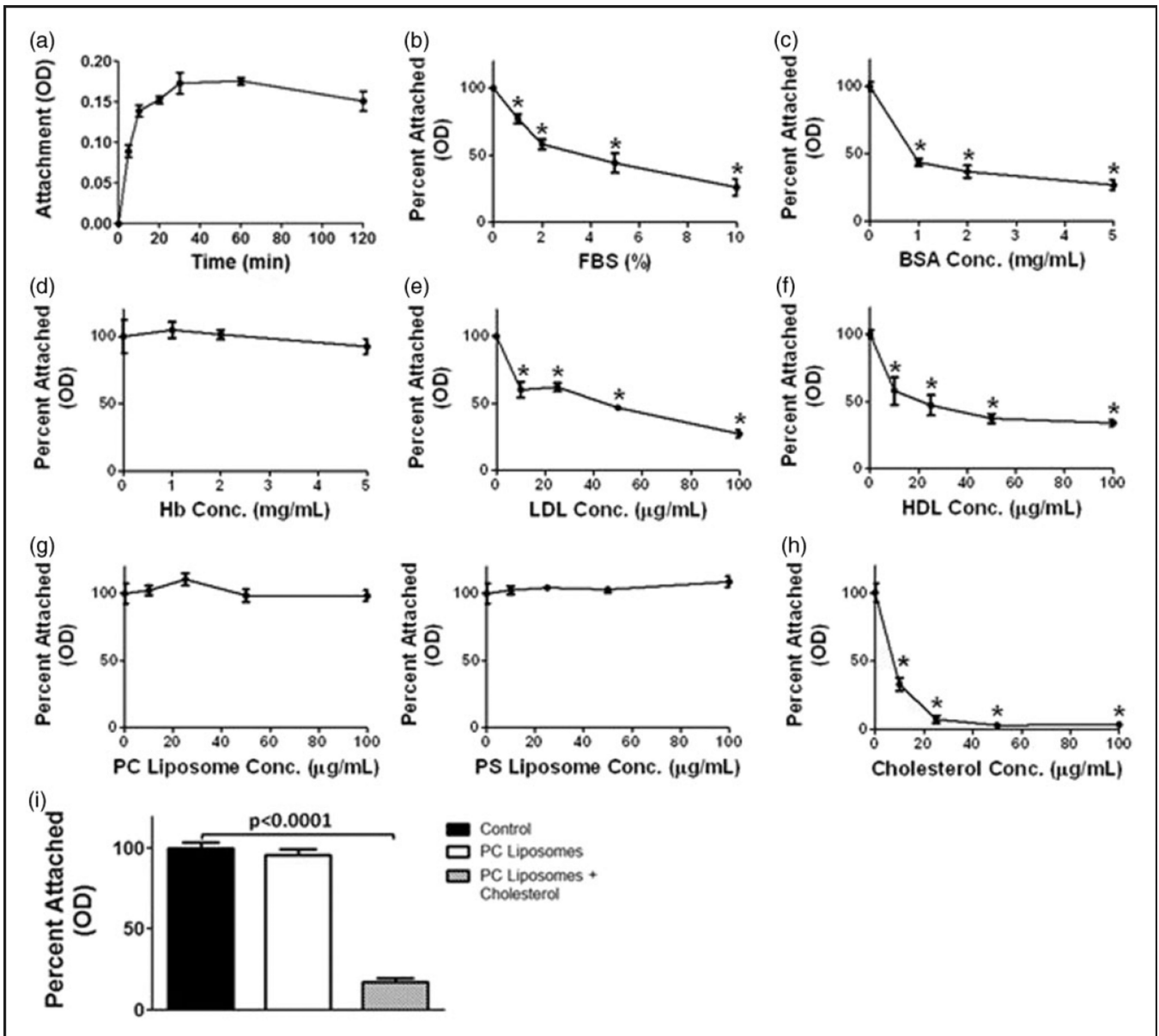
**Figure 3.**

Fc-mediated phagocytosis differs between the two morphologically different subpopulations. (a) BM-derived Mφs or (b) J774 cells were incubated ( $5 \times 10^5$  cells) with IgG-opsonized *E. coli* particles labeled with pHRodo (Life Technologies) at a ratio of 20:1 particles to cells for 1 h at both 4°C (negative control) and 37°C. The levels of phagocytosis were expressed as the geometric MFI. Experiments were performed in triplicate and repeated three times.



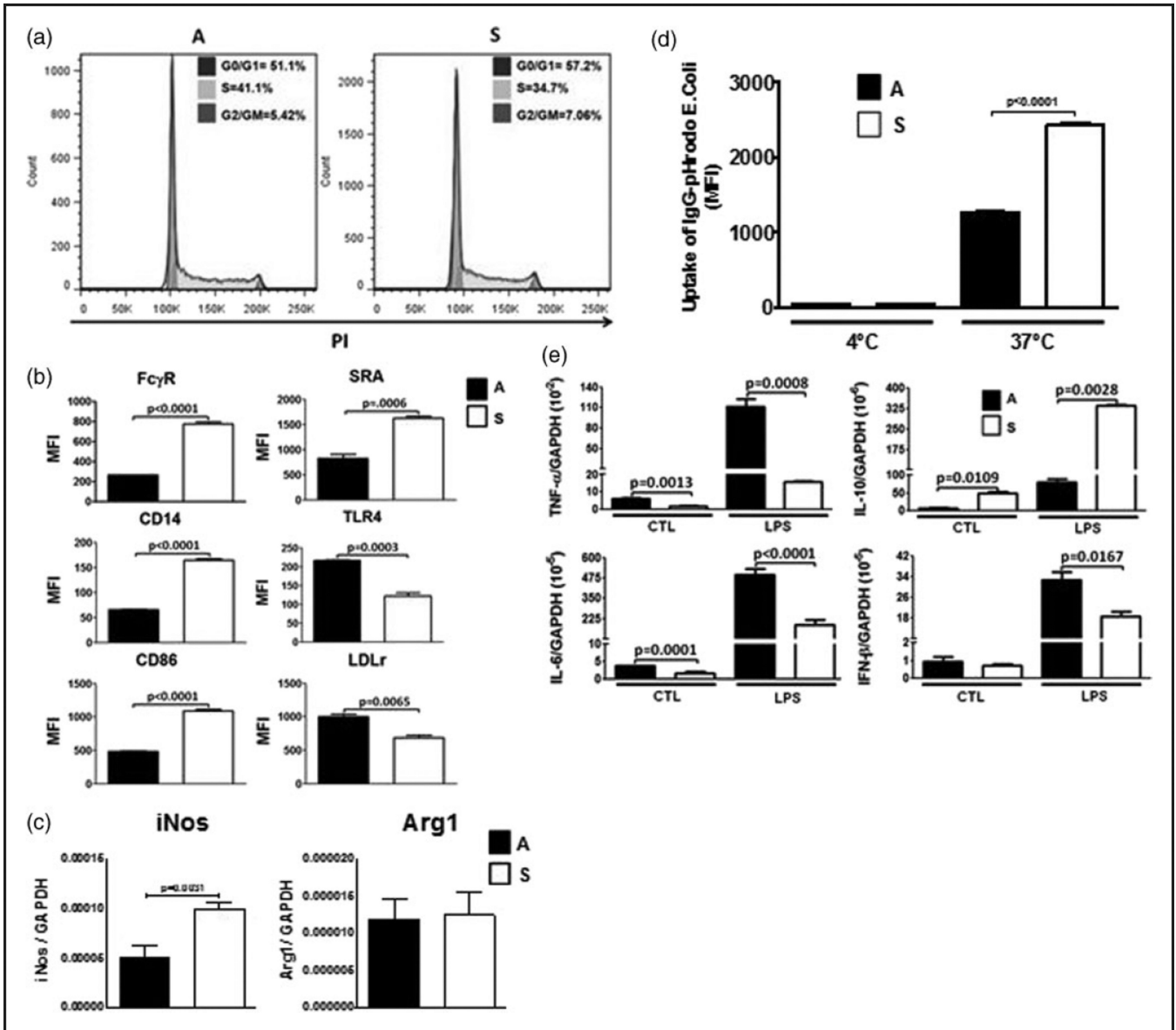
**Figure 4.**

Macrophage subpopulations were recapitulated by growing in different conditions. (a) Mφs (J774 cells) were grown in suspension on non-TC-treated plastic dishes in the presence of 10% FBS at 37°C, presenting a round morphology after staining with FITC-conjugated Ab against FcγR and visualized by fluorescent microscopy. (b) Removal of FBS (2 h, 37°C) resulted in rapid attachment of cells to the non-TC-treated plastic dishes, displaying a fibroblast-like morphology also visualized after staining with FITC-conjugated Ab against FcγR. The difference in size (FSC) between cells growing (c) in presence of serum or (d) in the absence of serum was documented by flow cytometry. For comparison, the shaded histograms (TC) correspond to the size of cells in TC dishes.



**Figure 5.**

Macrophages in suspension attach to plastic surfaces depending on the presence or serum in the medium. (a) J744 cells in suspension (S) were incubated in FBS-free medium at 37°C from 5 to 120 min, and the number of cells that attached to non-TC dishes was measured by the MTT method. S cells were incubated in the presence of various concentrations of (b) FBS, (c) BSA, (d) Hb, (e) LDL, (f) HDL, (g) PS liposomes, (h) PC liposomes and (i) water-soluble cholesterol. (i) Cells were also incubated with PC or cholesterol/PC-liposomes. The number of cells that attached to non-TC dishes was measured once again by the MTT method. Statistical analysis was determined from three independent experiments by both two-tailed *t*-tests and one-way ANOVA, and significance was accepted as  $P < 0.05$ .

**Figure 6.**

Suspension or attached A macrophages displayed different phenotype and function. (a) J774 cells in suspension (S) or attached (A) Mφs were analyzed for their differences in cell cycle, (b) expression of FcγR, CD14, Cd86, SRA, TLR4 and LDLr by flow cytometry, (c) mRNA expression of iNOS and Arg1 measured by qRT-PCR using GAPDH mRNA levels as housekeeping gene, (d) Fc-mediated phagocytosis and the response to LPS (1 ng/ml LPS for 2 h at 37°C). (e) Cytokine mRNA levels (TNF-α, IL-6, IL-10 and IFN-β) were measured by qRT-PCR using GAPDH mRNA levels to normalize the samples. Statistical analysis was determined by two-tailed *t*-tests from three independent experiments, and significance was accepted as  $P < 0.05$ . CTL: control.